Reactive Gas Environment Induced Structural Modification of Noble-Transition Metal Alloy Nanoparticles

V. Petkov,[1,*] L. Yang,[2] J. Yin,[2] R. Loukrakpam,[2] S. Shan,[2] B. Wanjala,[2] J. Luo,[2] K. W. Chapman,[3] and C. J. Zhong[2]

[1]*Department of Physics, Central Michigan University, Mt. Pleasant, Michigan 48859, USA*
[2]*Department of Chemistry, State University of New York at Binghamton, New York 13902, USA*
[3]*X-ray Science Division, Advanced Photon Source, Argonne National Laboratory, Argonne, Illinois 60439, USA*
(Received 17 June 2012; published 19 September 2012)

Noble-transition metal (noble = Pt, Au; transition = Co, Ni, Cu) alloy particles with sizes of about 5 nm have been studied by *in situ* high-energy x-ray diffraction while subjected to oxidizing (O_2) and reducing (H_2) gas atmospheres at elevated temperatures. The different gas atmospheres do not affect substantially the random alloy, face-centered-cubic structure type of the particles but do affect the way the metal atoms pack together. In an O_2 atmosphere, atoms get extra separated from each other, whereas, in an H_2 atmosphere, they come closer together. The effect is substantial, amounting to 0.1 Å difference in the first neighbor atomic distances, and concurs with a dramatic change of the particle catalytic properties. It is argued that such reactive gas induced "expansion shrinking" is a common phenomenon that may be employed for the engineering of "smart" nanoparticles responding advantageously to envisaged gas environments.

With current technology moving rapidly toward smaller scale, metallic systems have been increasingly produced in nanoscale dimensions and, by employing various postsynthesis techniques, have attempted to be further optimized, aiming at enhancing functional properties. The noble-transition metal (noble = Pt, Au; TM = Co, Ni, Cu) stands out as a particular system of interest because of its great potential for biomedical [1], optical [2], magnetic [3], and catalytic [4] applications. The unique functionality of nanosized metallic particles arises mostly from quantum size confinement effects that have a profound influence on their atomic-scale structure and, hence, physicochemical properties. However, nanosized particles (NPs) also have a very large surface-to-volume ratio and can interact with their environment. Evidence is emerging that, when the environment is condensed matter, such as liquid, for example, the interaction can be very substantial, including inducing extra strain and modifying the NP's atomic ordering [5]. A reactive gas environment has been shown to influence the surface chemistry of NPs [6], but little is known about its possible effect on the NP atomic-scale structure. Successful realization of nanotechnologies depends on good understanding of this effect, since NPs are often processed and/or used in reactive gas atmospheres.

In this Letter, we explore a particular application of noble-TM NPs as catalysts by using *in situ* high-energy x-ray diffraction (XRD) coupled to atomic pair distribution function analysis. The NPs are very stable chemically, allowing us to concentrate on the effect on the atomic-scale structure alone. We find that these NPs respond very strongly and differently to the different reactive gas atmospheres in which they are thermally treated. The packing of the metallic species across the particles loosens when they

are thermally treated in an O_2-rich atmosphere. On the other hand, the metal atoms come closer together when treated in a reducing, i.e., H_2-rich, atmosphere. Yet no detectable formation of bulk metal-oxide or hydride nanophases is observed in the respective cases. The NPs remain in their "expanded" and "compressed" states when taken out of the respective (O_2/H_2) gas environment and brought back to room temperature, indicating that the observed structural modifications are permanent. The expanded and compressed structure states of noble-TM NPs concur with profound differences in their catalytic performance, indicating a strong reactive gas environment induced—atomic-scale structure state—functional property relationship. This relationship is observed in a range of noble-TM NPs, suggesting that it does not depend much on the particular NP's chemistry and so is likely to be fairly universal in character. We argue that as such it has to be taken into account in nanocatalysts and other related areas of NP research.

The synthesis of the binary and ternary alloy NPs studied here followed well established methods involving the mixing of appropriate metal precursors in predefined ratios in solution [7]. Thiols/amines and oleic acid/oleylamine compounds were added to the organic solution as capping agents. Once cleaned from the synthesis reaction by-products, the NPs were mixed with carbon powder in solution. The resulting suspension of carbon supported NPs was dried in N_2. The NPs loading on carbon was 10 wt %. We prepared and studied several binary and ternary noble-TM alloy NPs. Exploring alloy NPs is essential, since noble metals, in particular Pt, although very useful in catalysis, are very scarce and so very limited for large-scale applications. Here, only the results for one ternary, $Pt_{25}Ni_{16}Co_{59}$, and one binary, $Au_{50}Cu_{50}$, system are reported. Note that other systems, such as $Pt_{39}Ni_{22}Co_{39}$

and $Pt_{45}V_{18}Co_{37}$, were also studied and found to show the reactive gas atmosphere-driven structural modification described here. Results for those systems will be reported elsewhere. The exact NP compositions were determined by direct current plasma-atomic emission spectroscopy. X-ray photoelectron spectroscopy (XPS) was also used to examine the NP surface chemical composition. The size and morphology of NPs was studied by transition electron microscopy (TEM). TEM results showed that the NPs studied here are spherical in shape and highly monodisperse, with an average size of about 5.2(5) nm. Exemplary TEM and XPS data are shown in the Supplemental Material as Figs. S1 and S2, respectively [8].

Typically, fresh synthesized NPs are subjected to extra thermal treatment to remove the organic molecules (amines and thiols, in our case) capping their surface and only then used in various, in particular, catalytic applications. Here, we followed two established protocols, namely, thermal treatment in oxidizing (80 vol % N_2 + 20 vol % O_2) and reducing (95 vol % N_2 + 5 vol % H_2) atmospheres. A sample cell, described and successfully tested in [9], was used.

In situ high-energy XRD data were collected on the beam line 11-ID-B, at the Advanced Photon Source, Argonne, using x rays of energy 90.48 keV ($\lambda = 0.1372$ Å). To improve the XRD data statistics, a large area detector was employed. Experimental diffraction patterns for $Pt_{25}Ni_{16}Co_{59}$ NPs are shown in Fig. 1. As can be seen in the figure, the XRD patterns show very broad diffraction features, a picture typical for nanosized materials. The peaks in the XRD patterns shift to higher Bragg angles when the sample is treated at 260 °C in an O_2 atmosphere for 30 min and remain shifted at those higher angles even after the sample is cooled back down to room temperature. When the gas atmosphere is changed to reducing (i.e., H_2), the peaks in the XRD patterns hardly shift in position, even though this time the sample is heated to considerably higher temperatures (400 °C). The peak shapes do not change substantially in either case. No new diffraction features appear, indicating no formation of new bulk nanophases. The very diffuse character of the Bragg peaks, however, makes it difficult to reveal the exact nature and magnitude of the structural changes taking place in the NPs when exposed to different reactive gas atmospheres. To alleviate the difficulty, the XRD data were reduced to their Fourier counterparts, the so-called atomic pair distribution functions (PDFs). High-energy XRD and atomic PDFs have already proven to be very efficient in studying the atomic ordering in NPs [10,11], including *in situ* studies of NPs during catalytic reactions [9,12].

The experimental PDFs for $Pt_{25}Ni_{16}Co_{59}$ NPs were approached with a structure model featuring an fcc-type atomic ordering that occurs in bulk noble and transition metals. As can be seen in Figs. 2(a) and 2(b), the experimental PDF data are almost perfectly fit by this model, showing that, as obtained and then exposed to different reactive gas
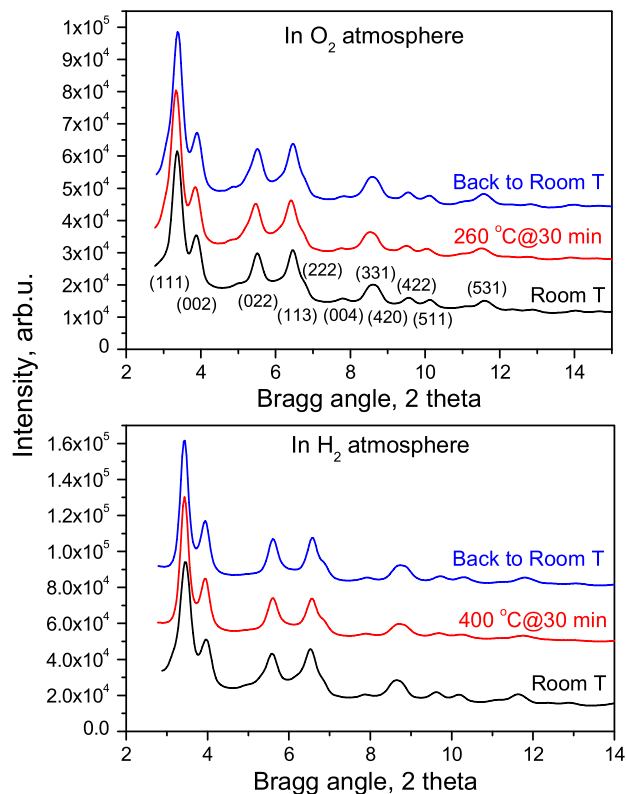

FIG. 1 (color online). Experimental XRD patterns for $Pt_{25}Ni_{16}Co_{59}$ NPs taken in O_2 and H_2 atmospheres. Also shown is the temperature at which the data were collected. Diffraction features have been tentatively assigned Miller indexes in a fcc lattice. The assignment, especially at higher Bragg angles, is highly ambiguous because of the features' heavy overlap.

environments, $Pt_{25}Ni_{16}Co_{59}$ NPs exhibit the same fcc-type atomic structure. No detectable amount of bulk metal-oxide or hydride nanophases is revealed by the PDF analysis, either. Some very fine features of the PDF data, in particular, a small peak at about 3.3 Å [see the arrow in Fig. 2(c)] signal the formation of metal-oxide-like and chemisorbed oxygen species on the very top surface of NPs treated in an O_2 atmosphere [12]. No such feature is observed in the PDF data for the sample treated in an H_2 atmosphere. What changes much more considerably is the way the metal atoms pack together. The fcc-lattice parameter of $Pt_{25}Ni_{16}Co_{59}$ NPs exposed to an O_2 environment changes from $a = 3.845$ Å to $a = 3.881$ Å at 260 °C and remains expanded at $a = 3.872$ Å, even when the sample is cooled back down to room temperature, indicating that this expansion is not merely due to the temperature increase but involves a permanent loosening of the atomic packing. When this sample is exposed to an H_2 atmosphere, the lattice parameter decreases from the initial value of $a = 3.872$ Å (at room temperature) to 3.788 Å at 400 °C, indicating a tightening of the atomic packing. Atoms in $Pt_{25}Ni_{16}Co_{59}$ NPs remain locked in this compressed state and, as expected, even come closer together
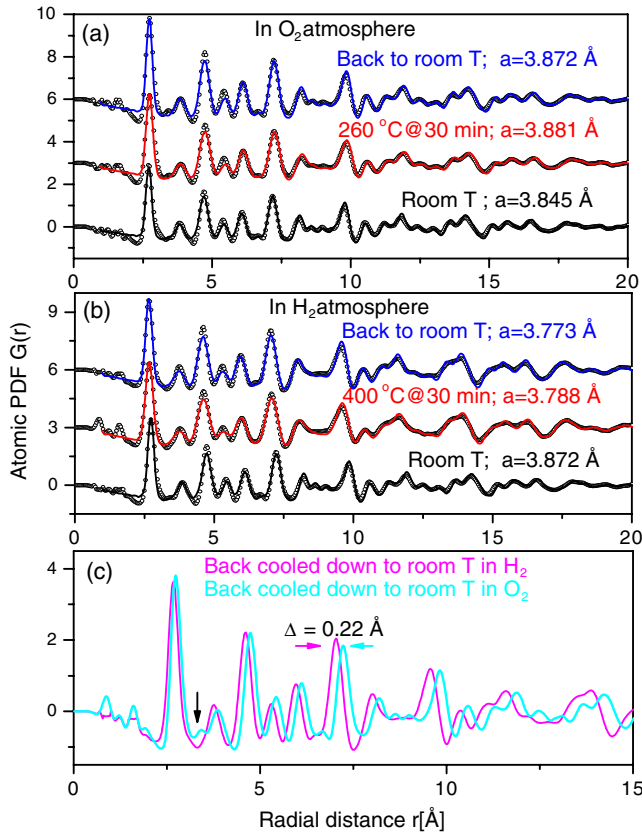
FIG. 2 (color online). Experimental (symbols) and model (solid line) atomic PDFs for $Pt_{25}Ni_{16}Co_{59}$ NPs. (a),(b) The refined fcc-lattice parameters are given by each data set. In (c), the experimental PDFs for samples treated in O_2 and H_2 atmospheres are compared to emphasize their different structural states. The vertical arrow marks a feature that may be associated with well expanded Pt-Pt distances due to the formation of metal-oxygen species at the NP surface [12].

when the sample is cooled down to room temperature ($a = 3.773$ Å). Overall, the average first neighbor metal-metal distance, as measured from the position of the first PDF peaks [see Fig. 2(c)], changes from 2.75 Å with the O_2 treated sample to 2.67 Å with the H_2 treated sample. The effect is cumulative, and, for example, the sixth neighbor interatomic distances appear at 7.22 and 7.01 Å, respectively, amounting to a difference of 0.22 Å [see Fig. 2(c)]. At the same time, no substantial change takes place in the NP bulk and surface (see the XPS data in the Supplemental Material [8]) chemical composition and NP shape. Obviously, the NPs remain fairly random noble-transition metal alloys, where atoms are arranged as in a fcc-type structure.

We observed a similar effect with binary $Au_{50}Cu_{50}$ NPs. The experimental atomic PDFs obtained in O_2 and H_2 atmospheres are shown in Fig. 3. Although the obtained $Au_{50}Cu_{50}$ NPs have a relatively low degree of crystallinity [see the fast decay of the PDF peaks above 10 Å in Fig. 3(a)], their atomic ordering can be very well approximated with a model featuring a single nanophase of a fcc-type structure
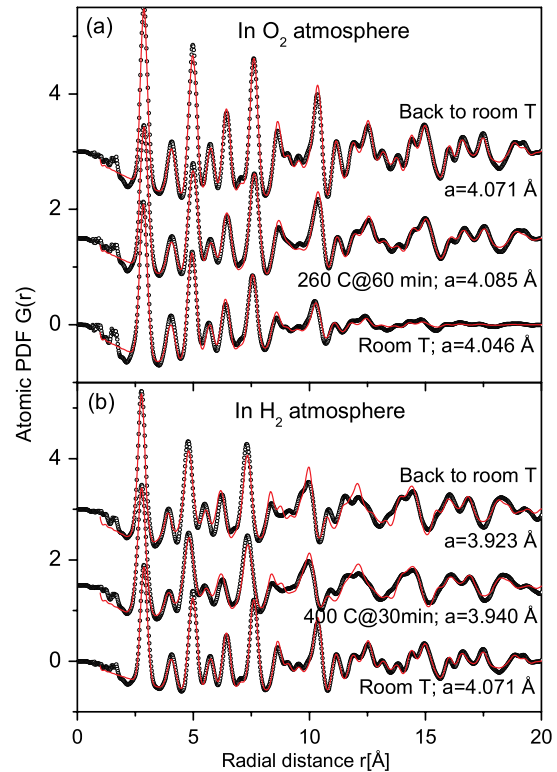

FIG. 3 (color online). Experimental (symbols) and model (solid line) atomic PDFs for $Au_{50}Cu_{50}$ NPs treated in (a) O_2 and (b) H_2 atmospheres. The refined fcc-lattice parameters are given by each data set.

with a lattice parameter of $a = 4.046$ Å. The NPs remain in a single nanophase and become more crystalline in nature when they are thermally treated in an O_2 atmosphere at 260 °C. The lattice parameter increases to $a = 4.085$ Å, and the fcc-type ordering remains loosened ($a = 4.071$ Å) when the sample is cooled back down to room temperature. When the gas atmosphere is changed to H_2 [see Fig. 3(b)], a tightening of the atomic packing is observed and preserved, as indicated by the trend in the refined lattice parameters: from 4.071 Å at room temperature to 3.940 Å at 400 °C and then to 3.923 Å when the sample is cooled back down to room temperature. Here, the average first neighbor metal-metal distance, as measured from the position of the first PDF peaks, changes from 2.86 Å with the O_2 treated sample to 2.76 Å with the H_2 treated sample. Obviously, due to their quite different electronegativity and reactivity, gas species like H_2 and O_2 interact very differently with the NP surface, including the formation of islands of metal-oxide-like and chemisorbed oxygen species on the very top surface of NPs exposed to O_2 [12,13]. No such species are likely to occur with H_2. The different interactions *propagate* into the NP interior, causing substantial strain (see Supplemental Figs. S5–S7 [8]), and are remarkably opposite in the trend of overall structural responses. A somewhat similar effect has been observed, with semiconductor NPs immersed in
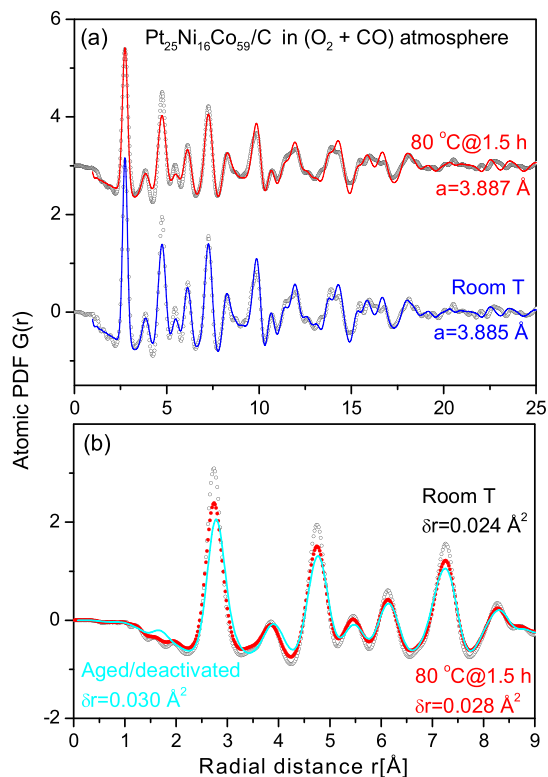
FIG. 4 (color online). Experimental (symbols) and model (solid line) atomic PDFs for (a) $Pt_{25}Ni_{16}Co_{59}$ NPs exposed to a mixture of O_2 and CO at room temperature and at $80\,^\circ$C for 1.5 h. Experimental PDFs of (a) are compared to those of $Pt_{25}Ni_{16}Co_{59}$ that have been subjected to a prolonged aging and so became catalytically inactive. (b) The rms atomic disorder, δr, is seen to increase with the catalyst aging time.

liquids of different polarity [5], but our results are the first clear observation with reactive gases.

The fact that NPs processed in an H_2 atmosphere are more compressed, i.e., have, on average, first interatomic distances shorter by ~0.1 Å than those in the O_2 atmosphere processed NPs, has a dramatic effect on the catalytic activity for a CO oxidation reaction in the gas phase and an oxygen reduction reaction (ORR) in electrolytes. For example, with the H_2 treated $Pt_{25}Ni_{16}Co_{59}$ NPs, the gas-phase CO conversion rate increases ~10 times and the mass activity for electrocatalytic ORR increases ~4 times: from 0.28 to 0.80 A/mg_{Pt} (see Supplemental Figs. S3 and S4, respectively [8]). These results are fully in line with theoretical predictions that shrinking of the metal-metal distances lowers the energy level of the d-band electrons with respect to the Fermi level and so decreases the binding energy of the CO species to the NP surface, substantially improving the catalytic activity [14]. These results are also consistent with the optimization of the binding energy of O_2 on the alloy catalyst [14] which consequently increases the electrocatalytic activity for ORR. In this respect, our study provides very strong and clear experimental evidence in support of these predictions.

The opposite process takes place during the CO oxidation reaction. The interaction of the O_2 and CO species with the NPs gradually increases the average metal-metal distances [seen as a shift in the first PDF peak in Fig. 4(b)] and also introduces extra strain and local structural disorder, resulting in asymmetry (see Supplemental Figs. S5–S7 [8]) and smearing [see Fig. 4(b)] of the PDF peaks. The effect is in line with theoretical predictions [13] and seen even if the NP catalyst has been used for 1.5 h only [see Fig. 4(a)] and the catalytic reaction temperature is as low as $80\,^\circ$C. Eventually, in time, the loosening of the interatomic packing, the extrastructural disorder, and the surface metal-oxide-like species pile up, rendering the NPs inactive as catalysts. Such an inactive catalyst, however, can be fully recovered by a thermal treatment in an H_2 atmosphere that not only would clean the NP surface from the metal-oxide-like species but, as our study shows, bring the metal atoms closer to interatomic separations that are more favorable for this catalytic reaction.

In summary, reactive gasses, like condensed matter, can interact strongly with noble-TM particles less than 10 nm in size, resulting in a substantial modification of the way the metallic species pack together. When being treated in an oxidizing atmosphere, the atomic packing of the NPs loosens, whereas, in a reducing atmosphere, the atomic packing gets tighter, without changing its random alloy fcc-structure-type character. The H_2 gas induced compressed structural state endows noble-TM NPs with much better catalytic properties. The considerable expansion or shrinking of the first and more distant interatomic distances observed here may also affect the optical and magnetic properties of NPs [15], and so the particular reactive gas environment should definitely, and more thoughtfully, be taken into account in NPs research. In particular, reactive gas environment induced structural modifications may offer new avenues for the engineering of smart metallic NPs for catalysis and other applications. One avenue to explore would be for NPs whose structure and, hence, structure-sensitive properties would be modified selectively and advantageously in response to envisaged changes in the gas-phase environment.

*Corresponding author
petkov@phy.cmich.edu

[1] Ch.-An. J. Lin, Ch.-H. Lee, J.-T. Hsiech, H. H. Wang, J. K. Li, J. L. Shen, W. H. Chan, H.-I. Yeh, and W. H. Chang, Jpn. J. Med. Electron. Biol. Eng. **29**, 276 (2009).
[2] P. Mulvaney, Langmuir **12**, 788 (1996).
[3] D. Alloyeau, C. Ricolleau, C. Mottet, T. Oitkawa, C. Langlois, Y. Le Bouar, N. Braidy, and A. Loiseau, Nature Mater. **8**, 940 (2009).
[4] P. Strasser, S. Koh, T. Anniyev, J. Greeley, K. More, Ch. Yu, Z. Liu, S. Kaya, D. Nordlund, H. Ogasawara, M. F. Toney, and A. Nillson, Nat. Chem. **2**, 454 (2010).

[5] H. Zhang, B. Chen, Y. Ren, G. A. Waychunas, and J. F. Banfield, Phys. Rev. B **81**, 125444 (2010); B. Gilbert, F. Huang, H. Zhang, G. A. Waychunas, and J. F. Banfield, Science **305**, 651 (2004).

[6] F. Tao, M. E. Grass, Y. Zhang, D. R. Butcher, J. R. Renzas, Zh. Liu, J. Y. Chung, B. S. Mun, M. Salmeron, and G. A. Somorjai, Science **322**, 932 (2008).

[7] M. J. Hostetler, C. J. Zhong, B. K. H. Yen, J. Anderegg, S. M. Gross, N. D. Evans, M. D. Porter, and R. W. Murray, J. Am. Chem. Soc. **120**, 9396 (1998); B. Wanjala, R. Loukrakpam, J. Luo, P. N. Njoki, D. Mott, M. Shao, L. Protsailo, T. Kawamura, and C. J. Zhong, J. Phys. Chem. C **114**, 17 580 (2010); B. Wanjala, B. Fang, R. Loukrakpam, Y. Chen, M. Engelhard, J. Luo, J. Yin, L. Yang, S. Shan, and C. J. Zhong, ACS Catalysis **2**, 806 (2012).

[8] See Supplemental Material at http://link.aps.org/supplemental/10.1103/PhysRevLett.109.125504 for TEM and catalytic properties data.

[9] P. J. Chupas, K. W. Chapman, Ch. Kurtz, J. C. Hanson, P. Lee, and C. P. Grey, J. Appl. Crystallogr. **41**, 822 (2008);

S. M. Oxford, P. L. Lee, P. J. Chupas, K. W. Chapman, M. C. Kung, and H. Kun, J. Phys. Chem. C **114**, 17 085 (2010).

[10] T. Egami and S. J. L. Billinge, *Underneath the Bragg Peaks* (Pergamon, Amsterdam, 2003).

[11] V. Petkov, Mater. Today **11**, 28 (2008).

[12] M. A. Newton, K. W. Chapman, D. Thompsett, and P. J. Chupas, J. Am. Chem. Soc. **134**, 5036 (2012).

[13] D. R. Butcher, M. E. Grass, Zh. Zeng, F. Aksoy, H. Bluhm, W.-X. Li, B. S. Mun, G. A. Somorjai, and Z. Liu, J. Am. Chem. Soc. **133**, 20 319 (2011); A. D. Allian, K. Takanabe, K. L. Fujdala, X. Hao, T. J. Truex, J. Cai, C. Buda, M. Neurock, and E. Iglesia, *ibid.* **133**, 4498 (2011).

[14] M. Mavrikakis, B. Hammer, and J. K. Norskov, PRLC newsletter **81**, 2819 (1998); M. O. Pedersen, S. Helveg, A. Ruban, I. Stensgaard, E. Laegsgaard, J. K. Norskov, and F. Besenbacher, Surf. Sci. **426**, 395 (1999); J. Greeley, I. E. L. Stephens, A. S. Bondarenko, T. P. Johansson, H. A. Hansen, T. F. Jaramillo, J. Rossmeisl, I. Chorkendorff, and J. K. Norskov, Nat. Chem. **1**, 552 (2009).

[15] A. Sun-Miguel, Chem. Soc. Rev. **35**, 876 (2006).